Characterization of Micellization Behavior of Amphiphilic Polymer Having Octadecyl Group by Small-Angle X-ray and Neutron Scattering

Minoru Nakano, Kozo Matsumoto, Hideki Matsuoka, and Hitoshi Yamaoka*

Department of Polymer Chemistry, Kyoto University, Kyoto 606-8501, Japan

Received October 26, 1998; Revised Manuscript Received March 24, 1999

ABSTRACT: Amphiphilic diblock polymers having an octadecyl group as a hydrophobic segment with different degrees of polymerization were synthesized by living cationic polymerization. Matrix-assisted laser desorption−ionization time-of-flight mass spectrometry (MALDI TOF MS) was performed to determine the molecular weight. Differential scanning calorimetry (DSC) measurements for polymer solid samples showed the melting point depending on the degree of polymerization. The size and shape of micelles formed by the polymers in water were investigated by small-angle X-ray scattering (SAXS) and neutron scattering (SANS) measurements. The aggregation number reduced with increasing degree of polymerization, while the overall micelle size was almost independent. The SAXS and SANS data revealed the sphere-to-disk transition on changing temperature for the polymer with the shortest hydrophilic chain. Below the melting point of hydrophobic chain, the polymer formed disklike aggregates with a crystallized core of octadecyl groups surrounded by a swollen shell. With increasing temperature, octadecyl groups melted and the spherical micelle formed.

Introduction

Amphiphiles, which show specific behavior such as micelle formation and adsorption in selective solvents, have attracted the attention of many research groups for a few decades.[1,2] Amphiphiles can be roughly divided into two groups, i.e., low molecular weight surfactants and polymer amphiphiles. For low molecular weight surfactants,[3] characterization of their self-assembly system is relatively simple because of no molecular weight distribution. However, since it is difficult to change the size of ionic headgroup of molecules, investigations of the effects of headgroups can be fulfilled only by changing the apparent size by variation of ionic strength in the system. On the other hand, the hydrophilic−lipophilic balance (HLB) of amphiphilic block copolymers[4−7] can be changed by control of the degrees of polymerization of both hydrophilic and hydrophobic segments, while molecular weight distribution yields ambiguity of phenomena and enhances the difficulty of characterization such as the determination of critical micellar concentration or micellar size.

Here, we introduce a new type of polymer amphiphile, which is synthesized by homopolymerization with an initiator having an octadecyl group. A constant length of hydrophobic chain is attainable by the initiator method, and the control of degree of polymerization corresponds to the control of headgroup size of the surfactant. Thus, this polymer has merits of both low molecular weight surfactants and polymer amphiphiles.

We have reported the micellization behavior of amphiphilic block copolymers having poly(2-hydroxyethyl vinyl ether (HOVE)) as a hydrophilic segment and formation of the anisotropic micelle.[8−10] The polymer that we present here has the same hydrophilic chain, and the degree of polymerization of HOVE can be precisely controlled by living cationic polymerization.[11,12]

Micelles of the surfactant with an octadecyl group have been little studied[13−16] because of the crystallinity with high melting point and poor solubility in water. However, sufficient hydrophilicity for dissolution can be supplied by an increase of the degree of polymerization. Moreover, such polymer surfactants must have an interesting micellization behavior near the melting point.

Herein, we studied the size and shape of the micelles formed by the amphiphilic polymer with an octadecyl group in water by the small-angle X-ray scattering (SAXS)[17,18] and neutron scattering (SANS)[19] techniques. The micellar shape was found to change from sphere to disk. This phenomenon is discussed along with differential scanning calorimetry (DSC) data.

Experimental Section

Synthesis. The amphiphilic polymers were prepared as shown in Scheme 1. The initiator having an octadecyl group was synthesized by bubbling of the hydrogen chloride gas into a hexane solution of octadecyl vinyl ether (ODVE, Tokyo Kasei, Tokyo). 2-Acetoxyethyl vinyl ether (AcOVE) was synthesized from sodium acetate (98.5%, Nacalai Tesque, Kyoto) and 2-chloroethyl vinyl ether (99%, Aldrich, Milwaukee, WI) at 90 °C. Commercial zinc chloride as diethyl ether solution (Aldrich) was used without further purification.

Living cationic polymerization was performed in a dried flask with three stopcocks under nitrogen. The hydrogen chloride adduct of ODVE and zinc chloride were injected as an initiator system in dichloromethane solution of AcOVE at −20 °C. The initial monomer/initiator molar ratio was changed to obtain four different molecular weight polymers (OD10, -20, -30, and -40, see Table 1). The polymerization was terminated by the addition of ammoniacal methanol.

After polymerization, AcOVE was led to water-soluble 2-hydroxyethyl vinyl ether (HOVE) by hydrolysis of the protective group with sodium hydroxide in dioxane. The obtained amphiphilic polymer ODVE−poly(HOVE) was purified by dialysis with deionized water. Their aqueous solutions were prepared by their direct dissolution into water and heated at 50 °C for 1 h. Then, they were passed through a filter with a pore size of 0.22 μm.

Molecular Characterization. Gel permeation chromatography (GPC) was carried out in chloroform on a Jasco 880-PU chromatograph equipped with four polystyrene gel columns

* To whom correspondence should be addressed.

10.1021/ma981675d CCC: $18.00
Published on Web 05/20/1999

Scheme 1. Synthesis of ODVE−Poly(HOVE)

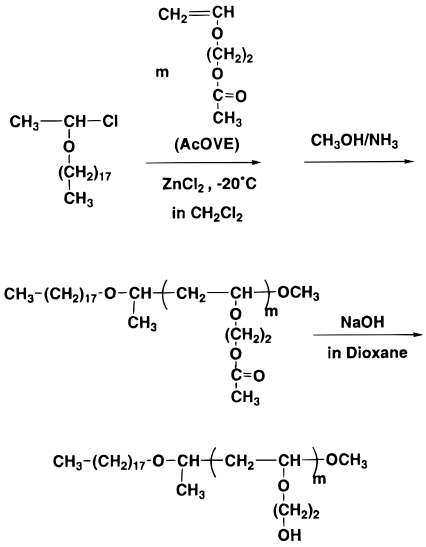

Table 1. Characterization of ODVE−Poly(HOVE)s and Their Micelles

	m_0/i_0[a]	m[b]	M_w/M_n[c]	shape	R_C	R_S	Φ_{disk}	N_{agg}
OD10	10	7.9	1.15	disk (25 °C)	20[d]	62[e]	0.2	
				sphere (45 °C)	28	50		167
OD20	20	16	1.18	sphere	20	50		61
OD30	30	28	1.21	sphere	16.5	53		34
OD40	40	34	1.23	sphere	15.5	56		28

[a] The initial monomer/initiator ratio. [b] Obtained by MALDI TOF MS. [c] By GPC before hydrolysis. [d] L_C. [e] L_S.

(Shodex K-802, K-803, K-804, and K-805) and a Jasco 830-RI refractive index detector. ^{1}H NMR spectra were obtained on a JEOL GSX 270 spectrometer. Matrix-assisted laser desorption−ionization time-of-flight mass spectrometry (MALDI TOF MS) was performed on a Shimadzu KOMPACT MALDI IV mass spectrometer using 3,5-dimethoxy-4-hydroxycinnamic acid (98%, Aldrich) as a matrix compound.

Differential Scanning Calorimetry (DSC). The DSC measurements were performed on a Thermal analyzer system WS002 (MAC Science, Tokyo) equipped with a TAPS1000S control unit and a DSC3100S module. Polymer solid samples (ca. 8 mg) were measured in an aluminum container under a dry nitrogen flow at heating or cooling rate of 10 °C/min. α-Alumina was used as a standard.

Small-Angle X-ray Scattering (SAXS). The SAXS measurements were performed using a Kratky type camera (Rigaku Corp., Tokyo) equipped with a rotating anode X-ray generator and a position sensitive proportional counter (PSPC). The SAXS instrument has been described in detail elsewhere.[20] Sample solutions were measured in glass capillaries (Mark, Berlin) with a diameter of 2 mm.

Small-Angle Neutron Scattering (SANS). The SANS measurements were performed by SANS-U of Institute for Solid State Physics, The University of Tokyo, at the research reactor JRR-3, Tokai, Japan. We used the wavelength (λ) of neutron source of 7 Å ($\Delta\lambda/\lambda = 10\%$). Solutions were measured in quartz cells (Nippon Silica Glass Co., Tokyo) with a pass length of 4 mm. Scattering data measured by a 2D detector were corrected for electronic background and circular averaged to be 1D form scattering data; then, the scattering of the empty cell was subtracted. The data were transformed to absolute cross sections using the Lupolen standard. From all scattering data of samples, we subtracted the scattering of solvent and the calculated incoherent scattering of the protonated portion of the polymer.

The SANS experiments for the OD10 solution were carried out at sample-to-detector distances of 1, 4, and 12 m, covering a range of the scattering vector (q) of $0.003 \le q \le 0.28$ Å^{-1}. For OD20 and OD30, the distance of 2 m was chosen to cover the range of $0.02 \le q \le 0.15$ Å^{-1}. We used D_2O as a solvent and a volume fraction of polymer of 1 vol % for all measurements.

Data Analysis of SAXS and SANS Measurements

A similar basic principle can be applied for both SAXS and SANS. The main difference is that the neutron is scattered by the density fluctuation of scattering length inherent for each atom, while the scattering of X-ray occurs by the electron density fluctuation.

When the contribution of interparticle interaction is negligible, the neutron scattering cross section can be given by the equation

$$d\Sigma(q)/d\Omega = n_p P(q) \quad (1)$$

where n_p is the number density of particles and $P(q)$ is the particle form factor including particle volume and density fluctuation terms. The scattering vector q is given by $q = 4\pi \sin\theta/\lambda$, where 2θ is the scattering angle and λ is the neutron wavelength.

Here we deal with the micelles in a core−shell structure. The particle form factor of a core−shell model can be written as follows:

$$P(q) = (1/2)\int_0^{\pi}\{(\rho_C - \rho_S)V_C F_C(q) + (\rho_S - \rho_0)V_S F_S(q)\}^2 \sin\beta \, d\beta \quad (2)$$

where ρ_C, ρ_S, and ρ_0 are the scattering length densities (for SANS) or electron densities (for SAXS) of the core, the shell, and the solvent. V_C and V_S are the volumes of the core and overall micelle, respectively. The scattering amplitude $F_i(q)$ (i = c, s) depends on the size and shape of the scattering particles.[17] For a core−shell sphere with a core radius of R_C and overall micelle size R_S (see Figure 10), $F_i(q)$ is given by

$$F_i(q) = 3(\sin(qR_i) - qR_i\cos(qR_i))/(qR_i)^3 \quad (3)$$

For a core−shell cylinder with a core radius of R_C and overall micelle size R_S and length L:

$$F_i(q) = \{(\sin(q(L/2)\cos\beta)/(q(L/2)\cos\beta)\} \times \{2J_1(qR_i\sin\beta)/(qR_i\sin\beta)\} \quad (4)$$

For a disklike structure with a core thickness of L_C, overall micelle size L_S, and radius R (see Figure 10)

$$F_i(q) = \{(\sin(q(L_i/2)\cos\beta)/(q(L_i/2)\cos\beta)\} \times \{2J_1(qR\sin\beta)/(qR\sin\beta)\} \quad (5)$$

β is the angle between the axis of symmetry of particle and the scattering vector q, and J_1 denotes the Bessel function of the first kind and of the order 1.

Results

Characterization of Amphiphilic Polymers. The number-averaged degree of polymerization of HOVE (m) was obtained by MALDI TOF MS. The polydispersity index M_w/M_n was determined for ODVE−poly(AcOVE) (before the hydrolysis) by GPC with polystyrene standard calibration, where M_w and M_n are the weight- and number-averaged molecular weights, respectively, since ODVE−poly(HOVE) was not soluble in chloroform. These values are listed in Table 1. Figure 1 shows

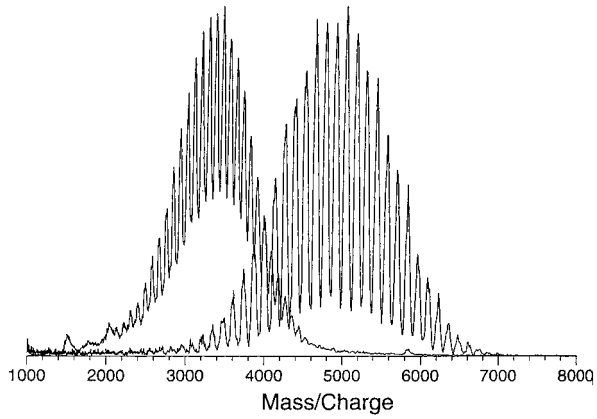

Figure 1. MALDI TOF MS spectra of OD40 and its precursor polymer.

MALDI TOF MS spectra of OD40 and its precursor polymer as typical examples. Observed peaks were quite sharp as can be seen in Figure 1, and the peak interval corresponded to the molecular weight of monomers (88 for ODVE−poly(HOVE) and 130 for ODVE−poly(AcOVE)). MALDI TOF MS is a quite effective technique to obtain the absolute molecular weight, but in the case of a diblock copolymer, it is not possible to obtain sharp peaks because of the chain length distributions of both segments. For the amphiphilic polymers we used, however, peaks were clearly found, and the molecular weight determination was possible, since these polymers had a hydrophobic chain with a fixed length introduced by the initiator method of living cationic polymerization. The obtained number-averaged degrees of polymerization of both HOVE and AcOVE were in agreement within 5% for all cases. This suggests that the hydrolysis was completed without any subreaction such as the polymer degradation process. We also confirmed by ^{1}H NMR that the octadecyl group was stable under the basic condition of hydrolysis.

DSC. The DSC curves of OD10, -20, -30, and -40 are shown in Figure 2a−d. In all cases, two endothermic peaks were observed in the heating curves. One peak that appeared at ca. 10 °C is probably due to the glass transition of poly(HOVE) and will not be discussed here. The other peak is more characteristic: It was observed at ca. 42 °C, and it became smaller with increasing hydrophilic chain length. This peak had a counterpart in the cooling curve, but the corresponding exothermic peak shifted to a lower temperature as the hydrophilic chain of the polymer became longer and disappeared as for OD30 and -40. This peak was attributed to the melting point of the octadecyl group. The increase of the hydrophilic chain length was considered to lower the degree of crystallinity, and the long hydrophilic chain prevents the octadecyl group from crystallizing during the cooling process. This thermal behavior of the polymers in a solid state is related to the properties of their micelles in an aqueous solution, which will be discussed later.

SAXS and SANS. The amphiphilic polymers OD20, -30, and -40 were dissolved in H_2O to prepare 1 wt % solutions for SAXS measurements. Direct dissolution with a smaller HOVE content made slightly turbid suspensions. However, they changed to transparent solutions by heating at 50 °C. These solutions were stable and kept their transparency at room temperature even after 1 month. For SANS measurements, a 1 vol % D_2O solution was prepared.

The SAXS profiles of the aqueous solutions of OD20−40 at room temperature are shown in Figure 3a−c. In all cases, a strong scattering was observed at a small angle, indicating the formation of large aggregates. In addition, a secondary maximum can be seen at $q \approx 0.1$ [Å^{-1}], implying a relatively narrow size distribution of micelles. The SANS profiles of D_2O solutions of OD20 and OD30 at room temperature are shown in Figure 4a,b. The secondary maximum near $q = 0.1$ was not observed in SANS curves. The difference of the scattering profiles between SAXS and SANS is evidence that micelles consist of the core−shell structure. In SANS experiments, the contrast between the core and the shell is considerably low compared with that between the shell and solvent. Then the scattering profile is similar to that of the homogeneous sphere. On the contrary, the electron density of the shell is higher than that of the core or the solvent, which yields the secondary maximum in the SAXS profile.

These scattering profiles were fitted by the form factor of spherical core−shell model with R_C and R_S as fitting parameters. By fitting the SANS profiles in an absolute scale we obtained the aggregation number of micelles, under the assumption of a close-packed core consisting of the hydrophobic initiator part of the polymer chain. The SAXS profiles in which the intensity is given on a relative scale were fitted by introduction of a shift factor. The value of the shift factor was kept constant while all the SAXS profiles were fitted. The fitting curves are shown in Figures 3 and 4 with the experimental data and the results in Table 1. The scattering at smaller angles and the position of secondary maximum are excellently reproduced by the fitting curve in all cases. The slight discrepancy for sharpness of the secondary maximum may be due to the polydispersity of micellar size. The deviation at larger angles is due to the low accuracy of the measured curves in this range and due to the fact that the scattering at larger angles is dominated by individual fluctuation of polymer chains in the shell (blobs), which was not considered in the core−shell model.

The aqueous solution of OD20 was also investigated at 45 °C by SAXS. The SAXS profiles at both room temperature and 45 °C show good agreement as can be seen in Figure 5, suggesting no temperature dependence of micellar shape and size in the temperature range studied here.

Different from OD20−40, the 1 wt % aqueous solution of OD10 was slightly turbid at room temperature and reversibly changed to transparent at a high temperature. Its SAXS profile at room temperature also exhibited a different tendency as shown in Figure 6. Although the position of the secondary maximum did not differ so much from that of the other polymer solutions, the intensity at a smaller angle decreased more abruptly with the increase of q, indicating the existence of larger aggregates. Figure 6 shows the qualitatively fitted results of the SAXS profile of OD10 by lines. The SAXS profile was first fitted by the form factor of a spherical core−shell model. However, the secondary maximum peak was not reproduced when a lower q region was fitted. In addition, spheres with smaller dimension that fit the secondary maximum could not show a satisfactory agreement at lower q angles. Then, a core−shell cylinder model was used, and it shifted the peak position to a higher q than that of spherical model when a lower q region was fitted, but it was still inadequate. Finally,

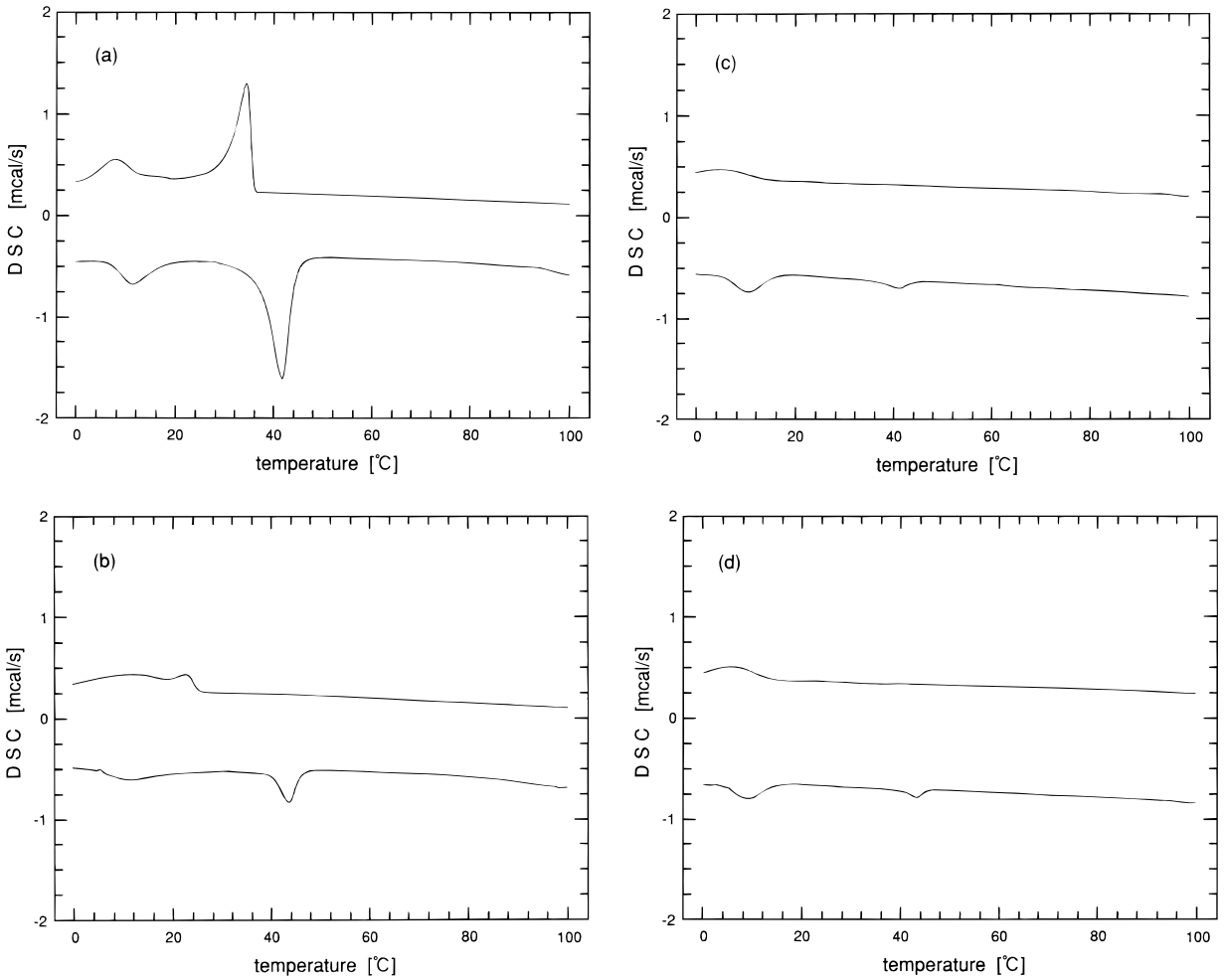

Figure 2. DSC curves of OD10 (a), OD20 (b), OD30 (c), and OD40 (d).

the agreement of both peak and a lower q region was achieved by introduction of a core−shell disk (or better to say sandwich-like) model. Thus, the existence of disklike aggregates was qualitatively proved, but quantitative fitting will be performed later.

The scattering intensity of disklike particles is proportional to q^{-2} at a small angle.[17] This scattering behavior could not be observed in the SAXS profile of OD10, since it was beyond the measurable q range. On the other hand, this behavior could be observed by SANS, which provides more information on smaller angle regions. Figure 7 shows the SANS profile of 1 vol % D_2O solution of OD10 at room temperature. The profile is quite different from the form factor of a sphere at smaller angles. However, the slope of the intensity at $q < 0.02$ [Å^{-1}] was less negative than that of a disk (−2). This means that the OD10 solution is not a system solely consisting of the disklike aggregates. It may indicate other shapes such as flexible rods (threadlike), branch, or network of rods, but it is more reasonable to consider that the disklike aggregates coexist with spherical micelles, if one takes into account the crystallization of octadecyl groups below the melting point.

The SANS measurement of D_2O solution of OD10 was also performed at 45 °C, which is higher than the melting point. A marked difference of the profiles between 25 and 45 °C can be seen in Figure 8. The profile of 45 °C resembled that of spherical micelles, since a flat region was observed at middle angle regions. Indeed, this profile could be fitted by the form factor of sphere with core−shell structure shown by the solid line in Figure 8. Deviation at a smaller angle might be due to a trace of large aggregates. The parameters are listed in Table 1. The solution was cooled to room temperature, and then SANS was performed again at 25 °C. The result was the same as obtained before heating, indicating the reversible change of the SANS profile and hence the reversible change of micelle structure.

Using both eqs 3 and 5, with introduction of the volume fraction of disklike aggregates Φ_{disk}, the SANS curve of 25 °C was well fitted as shown by the dotted line in Figure 8. The structure of the spherical micelles involved in the solution at 25 °C was assumed to be the same as that at 45 °C, and the volume fraction of disklike aggregates was determined to be 0.2 (20% disk and 80% sphere in volume). The values of L_C and L_S are also listed in Table 1. Although the value of the overall radius R of 300 Å was used, it is the smallest possible value, and the exact size of the disklike aggregates could not be determined, since the information about the total size is provided from a smaller q region than that covered in this experiment. With the same structure parameters as used for describing the SANS data of OD10, the SAXS curve was also well reproduced as shown in Figure 9.

Discussion

Spherical Micelle. The relationship between molecular architecture and structure of micelles can be clarified from SAXS and SANS results. If the structure

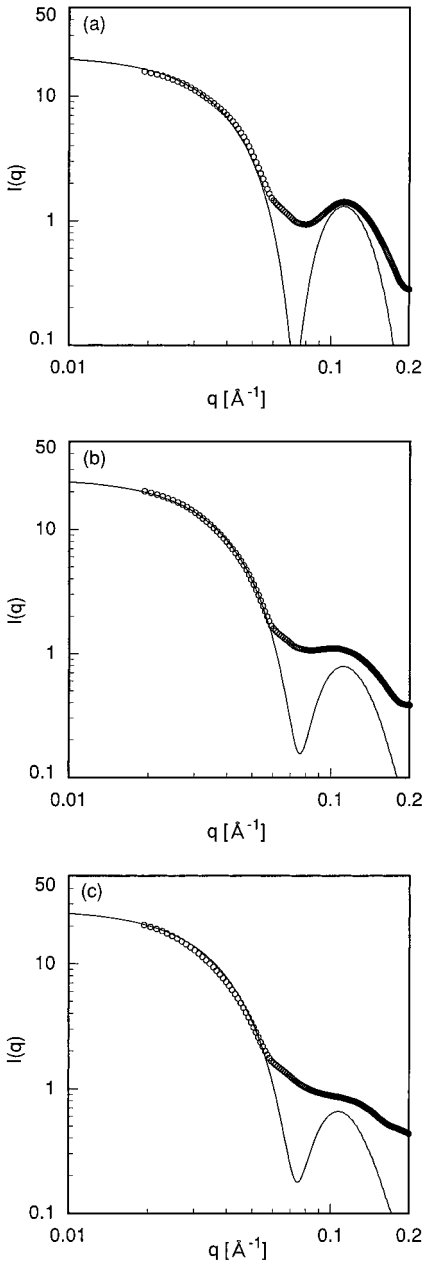

Figure 3. SAXS profiles of amphiphilic polymers in H_2O at 25 °C: OD20 (a), OD30 (b), and OD40 (c). Solid lines are theoretical curves of the spherical core−shell model.

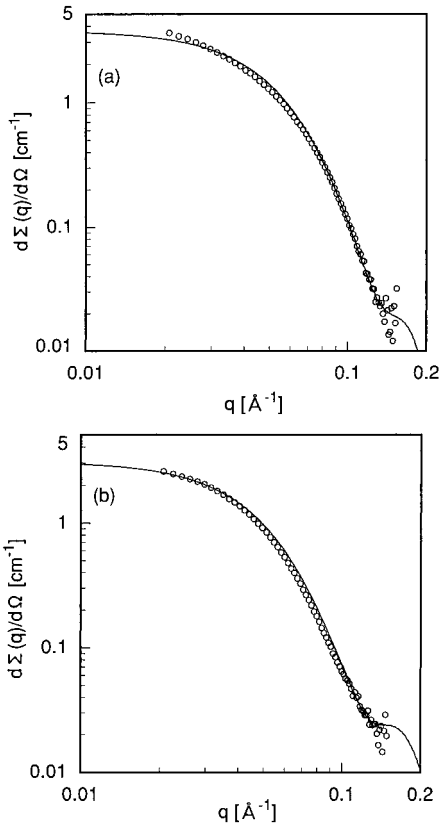

Figure 4. SANS profiles of D_2O solutions of OD20 (a) and OD30 (b). Solid lines are theoretical curves of the spherical core−shell model.

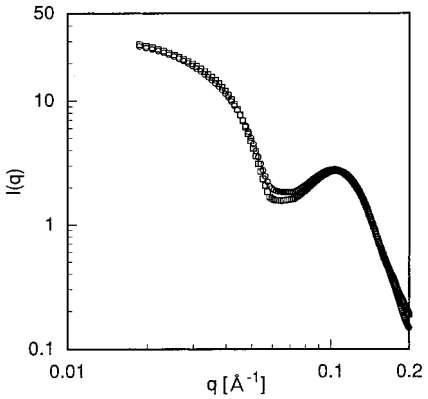

Figure 5. SAXS profiles of OD20 in H_2O at 25 °C (□) and 45 °C (○).

of the spherical micelles is assumed to be independent of temperature, the four different spherical micelles can be compared (Table 1). The polymer with a shorter hydrophilic chain forms micelles having a larger value of R_C (or N_{agg}), while R_S seems to be independent of the degree of polymerization (m). From the values listed in Table 1, we obtained the relation of $N_{agg} \propto m^{-1.31}$. The higher hydrophilicity given by the increase of m reduced the aggregation number. On the contrary, the size of overall micelle was little affected by the total length of polymer.

Sphere-to-Disk Transition. OD10, which is the polymer with the shortest hydrophilic chain, showed properties different from the others. It formed disklike aggregates at room temperature and reversibly changed into spherical micelles with increasing temperature. This transitional behavior can be interpreted by the DSC result. For OD10, the exothermic peak corresponding to the melting point observed on cooling was higher than that at room temperature (25 °C), in contrast with the other polymers that had exothermic peaks lower than those at room temperature or no peaks. From these results, we concluded that the structural transition of micelles is induced by the crystallization or melting of alkyl chains. Below the melting point, the polymer forms disklike aggregates with a crystallized core of octadecyl groups surrounded by a swollen HOVE shell, and spherical micelles are formed by the melting of the crystallized core at temperatures higher than the melting point.

The sphere-to-disk transition has been reported for octadecyltrimethyammonium bromide (C_{18}TAB) micelles with increasing salt concentration, and disklike micelles coexisting with globular micelles at a certain salt concentration have been observed by cryo-TEM

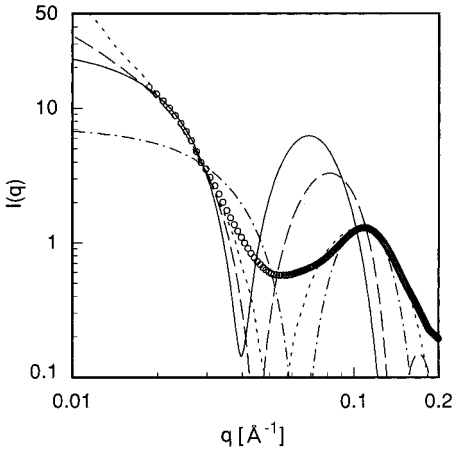

Figure 6. SAXS profile of OD10 in H_2O at 25 °C. The lines are theoretical curves of core−shell particles. Solid: sphere to reproduce low q region (R_C = 34 Å, R_S = 77 Å); dash−dot: sphere to reproduce maximum at high q region (R_C = 22 Å, R_S = 49 Å); broken: rod (R_C = 16 Å, R_S = 58 Å); dot: disk (L_C = 22 Å, L_S = 68 Å).

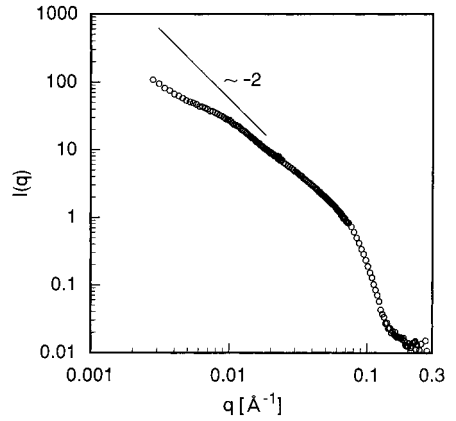

Figure 7. SANS profile of OD10 in D_2O at 25 °C.

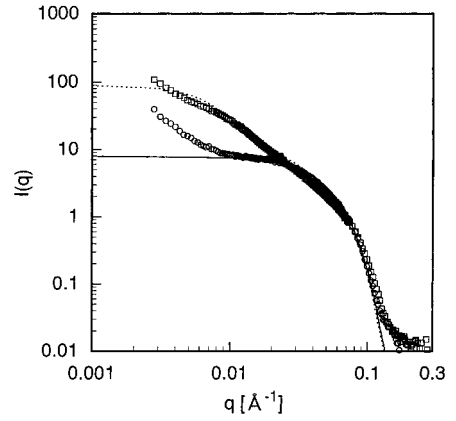

Figure 8. SANS profiles of OD10 in D_2O at 25 °C (□) and 45 °C (○). The solid line is the theoretical curve of the spherical core−shell model. The dotted line is based on the assumption of coexistence of spherical micelles and disklike aggregates with the volume fraction of disk of 0.2.

measurements.[14] This surfactant has an alkyl chain of the same length as the polymer we used. The increase of salt concentration shields the electrostatic repulsion between charged headgroups of C_{18}TAB globular micelles, which induces the transition to disklike structures. The same effect, i.e., a decrease of "effective" area of headgroup, can be introduced by reduction of hydrophilic chain length in the case of our polymer surfactants. Indeed, we observed the sphere-to-disk transition at room temperature when the degree of polymerization of HOVE was decreased.

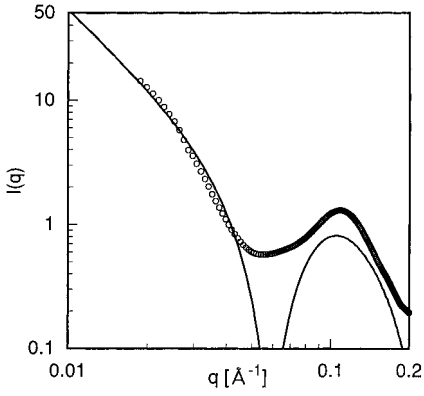

Figure 9. SAXS profiles of OD10 in H_2O at 25 °C, fitted by the same model as used for SANS.

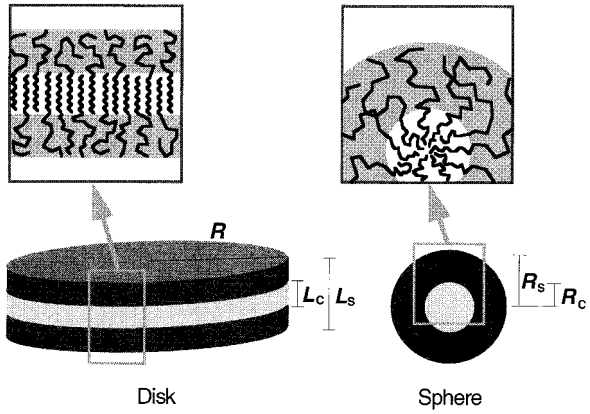

Figure 10. Schematic representation of the structures of spherical micelle and disklike aggregate. The crystallized alkyl chains form the core of a disk surrounded by swollen HOVE chains.

The internal structures of disk and spherical micelles predicted by the present systematic study are schematically shown in Figure 10. The polymers with a longer hydrophilic chain favor the spherical micelle formation because of the larger repulsion between hydrophilic chains. On the other hand, the disklike structure is favored for shorter chain polymers. For the disklike structure of C_{18}TAB, the core is considered to consist of a bilayer of octadecyl chains.[15] OD10, however, is supposed to have a crystallized monolayer core where octadecyl groups penetrate from both sides of the planar core as shown in Figure 10, if the relatively small value of L_C (20 Å) determined by SANS and SAXS is taken into account.

Conclusions

The amphiphilic polymers ODVE−poly(HOVE) were synthesized by living cationic polymerization and subsequent hydrolysis. The molecular weight determination by MALDI TOF MS was possible because of the fixed length of the hydrophobic chain. The size and shape of micelles formed by these polymers in water were investigated by SAXS and SANS measurements. The aggregation number was reduced with the increase in hydrophilic chain length, while the size of overall micelle was almost independent of the total length of polymer. In addition, the SAXS and SANS data showed a transition from disk to sphere with decreasing temperature

for the polymer with the shortest hydrophilic chain. This transition can be explained by the DSC data of the polymer in a solid state, which shows the melting point. We conclude that the disklike aggregates with crystallized core change into the spherical micelles by the melting of octadecyl groups with increasing temperature.

Acknowledgment. This work was supported by a Grant-in-aid from the Ministry of Education, Science, and Culture (No.09305062). Special thanks are due to Professor Y. Matsushita and Dr. M. Nagao for their kind help of SANS measurement at Tokai, which was adopted as the Proposal Number 98-107. M.N. gratefully acknowledges the support of this work by Research Fellowships of the Japan Society for the Promotion of Science for Young Scientists.

References and Notes

(1) Shah, O. D. *Micelles, Microemulsions, and Monolayers*; Marcel Dekker: New York, 1998.
(2) Tanford, C. *The Hydrophobic Effect: Formation of Micelles and Biological Membranes*, 2nd ed.; John Wiley: New York, 1980.
(3) Tadros, T. F. *Surfactants*; Academic Press: London, 1984.
(4) Halperin, A.; Tirrell, M.; Lodge, T. P. *Adv. Polym. Sci.* **1992**, *100*, 31.
(5) Chu, B. *Langmuir* **1995**, *11*, 414.
(6) Tuzar, Z.; Kratochvil, P. *Advances in Colloid and Interface Science*; Elsevier: Amsterdam, 1976.
(7) Zana, R. *Colloid Surf. A: Physicochem. Eng. Aspects* **1997**, *123−124*, 27.
(8) Yamaoka, H.; Matsuoka, H.; Sumaru, K.; Hanada, S.; Imai, M.; Wignall, G. D. *Physica B* **1995**, *213&214*, 700.
(9) Nakano, M.; Matsuoka, H.; Yamaoka, H.; Poppe, A.; Richter, D. *Physica B* **1998**, *241−243*, 1038.
(10) Nakano, M.; Matsuoka, H.; Yamaoka, H.; Poppe, A.; Richter, D. *Macromolecules* **1999**, *32*, 697.
(11) Sawamoto, M. *Prog. Polym. Sci.* **1991**, *16*, 111.
(12) Minoda, M.; Sawamoto, M.; Higashimura, T. *Macromolecules* **1987**, *20*, 2045.
(13) Kodama, M.; Seki, S. *Adv. Colloid Interface Sci.* **1991**, *35*, 1.
(14) Swanson-Vethamuthu, M.; Feitosa, E.; Brown, W. *Langmuir* **1998**, *14*, 1590.
(15) Kodama, M.; Tsujii, K.; Seki, S. *J. Phys. Chem.* **1990**, *94*, 815.
(16) von Berlepsch, H.; Mittelbach, R.; Hoinkis, E.; Schnablegger, H. *Langmuir* **1997**, *13*, 6032.
(17) Guinier, A.; Fournet, G. *Small-Angle Scattering of X-rays*; John Wiley: New York, 1955.
(18) Glatter, O.; Kratky, O. *Small-Angle X-ray Scattering*; Academic Press: London, 1982.
(19) Higgins, J. S.; Benoit, H. C. *Polymers and Neutron Scattering*; Oxford: New York, 1994.
(20) Ise, N.; Okubo, T.; Kunugi, S.; Matsuoka, H.; Yamamoto, K.; Ishii, Y. *J. Chem. Phys.* **1984**, *81*, 3294.

MA981675D